Research Article Vol. 26, No. 7 | 2 Apr 2018 | OPTICS EXPRESS 9011

Optics EXPRESS

$Ho:KY(WO_4)_2$ thin-disk laser passively Q-switched by a GaSb-based SESAM

XAVIER MATEOS,[1,2,3,*] PAVEL LOIKO,[4] SAMIR LAMRINI,[3] KARSTEN SCHOLLE,[3] PETER FUHRBERG,[3] SOILE SUOMALAINEN,[5] ANTTI HÄRKÖNEN,[5] MIRCEA GUINA,[5] SERGEI VATNIK,[6] IVAN VEDIN,[6] MAGDALENA AGUILÓ,[2] FRANCESC DÍAZ,[2] YICHENG WANG,[1] UWE GRIEBNER,[1] AND VALENTIN PETROV[1]

[1]*Max Born Institute for Nonlinear Optics and Short Pulse Spectroscopy, Max-Born-Str. 2a, D-12489 Berlin, Germany*
[2]*Física i Cristal·lografia de Materials i Nanomaterials (FiCMA-FiCNA)-EMaS, Dept. Química Física i Inòrganica, Universitat Rovira i Virgili (URV), Campus Sescelades, E-43007 Tarragona, Spain*
[3]*LISA Laser Products OHG, Max-Planck-Str. 1, D-37191 Katlenburg-Lindau, Germany*
[4]*ITMO University, 49 Kronverkskiy Pr., 197101 St. Petersburg, Russia*
[5]*Optoelectronics Research Centre, Tampere University of Technology, PO Box 692, 33101 Tampere, Finland*
[6]*Institute of Laser Physics, Siberian Branch of Russian Academy of Sciences, 13/3 Lavrentyev Ave, 630090 Novosibirsk, Russia*
[*]*xavier.mateos@urv.cat*

Abstract: A Holmium thin-disk laser based on a 3 at.% $Ho:KY(WO_4)_2$ / $KY(WO_4)_2$ epitaxy and single-bounce pumping by a 1960 nm Tm-fiber laser is passively Q-switched with a GaSb-based quantum-well semiconductor saturable absorber mirror. It generates an average output power of 551 mW at 2056 nm with a slope efficiency of 44% (with respect to the absorbed pump power). The best pulse characteristics (energy and duration) are 4.1 μJ / 201 ns at a repetition rate of 135 kHz and the conversion efficiency with respect to the continuous-wave regime is as high as 93%.

© 2018 Optical Society of America under the terms of the OSA Open Access Publishing Agreement

OCIS codes: (140.3380) Laser materials; (140.3540) Lasers, Q-switched; (140.3070) Infrared and far-infrared lasers.

References and links

1. A. Giesen, H. Hügel, A. Voss, K. Wittig, U. Brauch, and H. Opower, "Scalable concept for diode-pumped high-power solid-state lasers," Appl. Phys. B **58**(5), 365–372 (1994).
2. A. Giesen and J. Speiser, "Fifteen years of work on thin-disk lasers: results and scaling laws," IEEE J. Sel. Top. Quantum Electron. **13**(3), 598–609 (2007).
3. C. J. Saraceno, F. Emaury, C. Schriber, A. Diebold, M. Hoffmann, M. Golling, T. Südmeyer, and U. Keller, "Toward millijoule-level high-power ultrafast thin-disk oscillators," IEEE J. Sel. Top. Quantum Electron. **21**(1), 106–123 (2015).
4. R. Peters, C. Kränkel, K. Petermann, and G. Huber, "Broadly tunable high-power $Yb:Lu_2O_3$ thin disk laser with 80% slope efficiency," Opt. Express **15**(11), 7075–7082 (2007).
5. T. Südmeyer, C. Kränkel, C. R. E. Baer, O. H. Heckl, C. J. Saraceno, M. Golling, R. Peters, K. Petermann, G. Huber, and U. Keller, "High-power ultrafast thin disk laser oscillators and their potential for sub-100-femtosecond pulse generation," Appl. Phys. B **97**(2), 281–295 (2009).
6. O. Pronin, J. Brons, C. Grasse, V. Pervak, G. Boehm, M.-C. Amann, V. L. Kalashnikov, A. Apolonski, and F. Krausz, "High-power 200 fs Kerr-lens mode-locked Yb:YAG thin-disk oscillator," Opt. Lett. **36**(24), 4746–4748 (2011).
7. F. Brunner, T. Südmeyer, E. Innerhofer, F. Morier-Genoud, R. Paschotta, V. E. Kisel, V. G. Shcherbitsky, N. V. Kuleshov, J. Gao, K. Contag, A. Giesen, and U. Keller, "240-fs pulses with 22-W average power from a mode-locked thin-disk $Yb:KY(WO_4)_2$ laser," Opt. Lett. **27**(13), 1162–1164 (2002).
8. E. Innerhofer, T. Südmeyer, F. Brunner, R. Häring, A. Aschwanden, R. Paschotta, C. Hönninger, M. Kumkar, and U. Keller, "60-W average power in 810-fs pulses from a thin-disk Yb:YAG laser," Opt. Lett. **28**(5), 367–369 (2003).
9. S. Ricaud, A. Jaffres, K. Wentsch, A. Suganuma, B. Viana, P. Loiseau, B. Weichelt, M. Abdou-Ahmed, A. Voss, T. Graf, D. Rytz, C. Hönninger, E. Mottay, P. Georges, and F. Druon, "Femtosecond $Yb:CaGdAlO_4$ thin-disk oscillator," Opt. Lett. **37**(19), 3984–3986 (2012).
10. J. Speiser, G. Renz, and A. Giesen, "Thin disk laser in the 2 μm wavelength range," Proc. SPIE **8547**, 85470E (2012).

#319767 https://doi.org/10.1364/OE.26.009011
Journal © 2018 Received 16 Jan 2018; revised 27 Feb 2018; accepted 28 Feb 2018; published 28 Mar 2018

11. M. Schellhorn, "Performance of a Ho:YAG thin-disc laser pumped by a diode-pumped 1.9 μm thulium laser," Appl. Phys. B **85**(4), 549–552 (2006).
12. D. Y. Shen, A. Abdolvand, L. J. Cooper, and W. A. Clarkson, "Efficient Ho:YAG laser pumped by a cladding-pumped tunable Tm:silica-fibre laser," Appl. Phys. B **79**(5), 559–561 (2004).
13. Y. Wang, G. Xie, X. Xu, J. Di, Z. Qin, S. Suomalainen, M. Guina, A. Härkönen, A. Agnesi, U. Griebner, X. Mateos, P. Loiko, and V. Petrov, "SESAM mode-locked Tm:CALGO laser at 2 μm," Opt. Mater. Express **6**(1), 131–136 (2016).
14. V. Aleksandrov, A. Gluth, V. Petrov, I. Buchvarov, G. Steinmeyer, J. Paajaste, S. Suomalainen, A. Härkönen, M. Guina, X. Mateos, F. Díaz, and U. Griebner, "Mode-locked Tm,Ho:KLu(WO_4)$_2$ laser at 2060 nm using InGaSb-based SESAMs," Opt. Express **23**(4), 4614–4619 (2015).
15. A. Gluth, Y. Wang, V. Petrov, J. Paajaste, S. Suomalainen, A. Härkönen, M. Guina, G. Steinmeyer, X. Mateos, S. Veronesi, M. Tonelli, J. Li, Y. Pan, J. Guo, and U. Griebner, "GaSb-based SESAM mode-locked Tm:YAG ceramic laser at 2 μm," Opt. Express **23**(2), 1361–1369 (2015).
16. Y. Wang, R. Lan, X. Mateos, J. Li, C. Li, S. Suomalainen, A. Härkönen, M. Guina, V. Petrov, and U. Griebner, "Thulium doped LuAG ceramics for passively mode locked lasers," Opt. Express **25**(6), 7084–7091 (2017).
17. Y. Wang, R. Lan, X. Mateos, J. Li, C. Hu, C. Li, S. Suomalainen, A. Härkönen, M. Guina, V. Petrov, and U. Griebner, "Broadly tunable mode-locked Ho:YAG ceramic laser around 2.1 μm," Opt. Express **24**(16), 18003–18012 (2016).
18. J. Paajaste, S. Suomalainen, A. Härkönen, U. Griebner, G. Steinmeyer, and M. Guina, "Absorption recovery dynamics in 2 μm GaSb-based SESAMs," J. Phys. D Appl. Phys. **47**(6), 065102 (2014).
19. J. Paajaste, S. Suomalainen, R. Koskinen, A. Härkönen, G. Steinmeyer, and M. Guina, "GaSb-based semiconductor saturable absorber mirrors for mode-locking 2 μm semiconductor disk lasers," Phys. Status Solidi **9**(2), 294–297 (2012).
20. V. Petrov, M. C. Pujol, X. Mateos, O. Silvestre, S. Rivier, M. Aguilo, R. Sole, J. Liu, U. Griebner, and F. Diaz, "Growth and properties of KLu(WO_4)$_2$, and novel ytterbium and thulium lasers based on this monoclinic crystalline host," Laser Photonics Rev. **1**(2), 179–212 (2007).
21. V. Jambunathan, X. Mateos, M. C. Pujol, J. J. Carvajal, F. Díaz, M. Aguiló, U. Griebner, and V. Petrov, "Continuous-wave laser generation at ~2.1 μm in Ho:KRE(WO_4)$_2$ (RE = Y, Gd, Lu) crystals: a comparative study," Opt. Express **19**(25), 25279–25289 (2011).
22. V. Jambunathan, X. Mateos, P. A. Loiko, J. M. Serres, U. Griebner, V. Petrov, K. V. Yumashev, M. Aguiló, and F. Díaz, "Growth, spectroscopy and laser operation of Ho:KY(WO_4)$_2$," J. Lumin. **179**, 50–58 (2016).
23. V. Jambunathan, X. Mateos, M. C. Pujol, J. J. Carvajal, C. Zaldo, U. Griebner, V. Petrov, M. Aguiló, and F. Díaz, "Crystal growth, optical spectroscopy, and continuous-wave laser operation of Ho:KLu(WO_4)$_2$ crystals," Appl. Phys. B **116**(2), 455–466 (2014).
24. S. Vatnik, I. Vedin, M. Segura, X. Mateos, M. C. Pujol, J. J. Carvajal, M. Aguiló, F. Díaz, V. Petrov, and U. Griebner, "Efficient thin-disk Tm-laser operation based on Tm:KLu(WO_4)$_2$/KLu(WO_4)$_2$ epitaxies," Opt. Lett. **37**(3), 356–358 (2012).
25. X. Mateos, S. Lamrini, K. Scholle, P. Fuhrberg, S. Vatnik, P. Loiko, I. Vedin, M. Aguiló, F. Díaz, U. Griebner, and V. Petrov, "Holmium thin-disk laser based on Ho:KY(WO_4)$_2$/KY(WO_4)$_2$ epitaxy with 60% slope efficiency and simplified pump geometry," Opt. Lett. **42**(17), 3490–3493 (2017).
26. R. Lan, P. Loiko, X. Mateos, Y. Wang, J. Li, Y. Pan, S. Y. Choi, M. H. Kim, F. Rotermund, A. Yasukevich, K. Yumashev, U. Griebner, and V. Petrov, "Passive Q-switching of microchip lasers based on Ho:YAG ceramics," Appl. Opt. **55**(18), 4877–4887 (2016).

1. Introduction

The thin-disk (also called active mirror) laser architecture [1] consists of a disk-shaped active element. Its rear face is in thermal contact with a bulk heat-sink. The heat flow in the disk in predominantly unidirectional (towards the cooling surface). The rear face of the disk has a dielectric coating reflecting both the pump and laser radiations serving as a cavity mirror. The laser radiation is propagating almost perpendicular to the disk surface. The thin-disk laser (TDL) design is promising for power-scalable and efficient laser sources operating in the continuous-wave (CW) and mode-locked (ML) regimes [2,3]. Typically, the thickness of the active element t is significantly smaller than the pump spot size ($t < 2w_p$) which is matched to the laser mode. A large pump spot size is favoring weak thermo-optic aberrations. Small thickness of the laser element (and, hence, low losses and nonlinear effects) is advantageous for reaching high efficiency in the CW regime [4] and stable ML operation [5].

High-power and highly-efficient TDLs at ~1 μm (based on Yb^{3+} ion doping) operating in the CW and ML regimes have reached a high level of maturity reflected in many leading scientific results and commercial products [4,6–9]. In the ML regime, semiconductor saturable absorber mirrors (SESAMs) are typically used [3,5]; these are commercially available and show attractive properties, e.g. ultrafast recovery time, low non-saturable losses, acceptable laser-induced damage threshold (LIDT) and versatility in

Optics EXPRESS

tailoring these parameters [5]. On the other hand, at ~2 μm (for Tm^{3+} and Ho^{3+} doped materials), the development stage is still in an early phase with sporadic reports on such laser sources in the literature, e.g., mainly reporting on CW Ho TDLs [10,11]. Moreover, the pulsed operation of ~2 μm TDLs is complicated by the lack of reliable SESAMs. However, pulsed (passively Q-switched (PQS) and ML) ~2 μm lasers are of interest for a wide range of applications in medicine, range-finding, environmental sensing and spectroscopy. This is in particular true for the Ho^{3+} ion emission above 2 μm related to the $^5I_7 \rightarrow {}^5I_8$ transition [12].

Recently, GaSb-based SESAMs containing few InGaSb quantum wells (QWs) were used as ultrafast saturable absorbers for bulk Tm and Ho lasers emitting above 2 μm, based on Tm:CALGO and Tm,Ho:KLuW crystals [13,14] and Tm:YAG, Tm:LuAG and Ho:YAG ceramics [15–17], and covering a broad spectral range extending from 2010 to 2120 nm. In particular, the ML Tm:CALGO laser generated pulses as short as 650 fs at a repetition rate of 100 MHz [13]. The effect of the growth temperature, QW location and the dielectric coating on the recovery time of GaSb-based SESAMs was reported in [18,19].

In the present work, we demonstrate the first PQS Ho thin-disk laser based on $Ho:KY(WO_4)_2$ (Ho:KYW) using a GaSb-based SESAM. The host crystal, KYW, belongs to the family of monoclinic double tungstates (MDTs). These crystals are known to be excellent hosts for rare-earth ions, e.g. Yb^{3+}, Tm^{3+}, Ho^{3+} [20,21]. Ho:MDTs provide high transition cross-sections for polarized light, broad spectral bands, relatively long lifetimes of the upper laser level and the possibility to dope at high concentrations [21–23]. To prepare Ho:KYW for a thin-disk fabrication, we used the liquid phase epitaxy (LPE) method. For MDTs, LPE is capable of producing high-optical-quality laser-active films with a thickness of few hundreds of μm on bulk undoped substrates, e.g., as demonstrated before for Tm^{3+} [24] and Ho^{3+} ions [25]. The high absorption cross-sections and moderate available doping levels of Ho^{3+} ions in LPE-grown KYW films allowed us to simplify the pump geometry to a single-bounce. In [25], the first Ho:KYW thin-disk laser generated 1.01 W at 2057 nm with a slope efficiency of 60% (for a single-bounce pumping).

2. Experimental

The scheme of the TDL set-up is shown in Fig. 1. The laser element consisted of a 3 at. % Ho:KYW LPE grown active layer (thickness $t = 250 \pm 10$ μm, $N_{Ho} = 2.16 \times 10^{20}$ cm^{-3}) on an (010)-oriented 1 mm-thick undoped KYW substrate (with ***b***-axis perpendicular to its surface) [25]. Both faces of the Ho:KYW / KYW epitaxy were polished to laser-grade quality. The substrate face was antireflection (AR) coated for 1800-2100 μm. The face with the Ho:KYW layer was coated for high reflection (HR) at 1800-2100 nm and then soldered to a Cu heat-sink that was water-cooled to 12 °C.

Ho:KYW is very suitable for the design of TDLs due to the high absorption cross-sections, $\sigma_{abs}(m) = 2.2$ and $\sigma_{abs}(g) = 0.76 \times 10^{-20}$ cm^2 at 1960 nm for light polarizations $E \parallel N_m$ and N_g, respectively (both accessible with a ***b***-cut laser element). The long lifetime of the upper laser level ($^5I_7$), $\tau_{Ho} = 4.8$ ms [22], means long energy storage in PQS operation. The high absorption cross-sections are normally associated with high emission cross-sections, $\sigma_{SE}(m) = 2.5 \times 10^{-20}$ cm^2 at 2056.5 nm for Ho:KYW which means easier saturation of the laser medium. Hence, employing a fast saturable absorber with yet lower saturation fluence as the present SESAM, PQS at repetition rates much higher than the inverse lifetime can be only expected.

A Z-shaped laser cavity was constructed, consisting of a concave output coupler (OC) having a transmission $T_{OC} = 3\%$ at 1800-2100 nm and a radius of curvature RoC of 75 mm, the flat HR-coated face of the laser element serving as a folding mirror (beam angle with the normal: 7°), and a concave HR mirror (RoC = 50 mm) to focus the laser beam on the SESAM. For CW operation, the SESAM was replaced by a flat HR mirror. The distances between the mirrors are indicated in Fig. 1, the physical cavity length L_{cav} amounted to 175 mm. The sensitivity factors of the thermal lens ($M = dD/dP_{abs}$, where D is the optical power of the lens and P_{abs} is the absorbed pump power) for a 3 at.% Ho:KYW / KYW epitaxy are measured to $M_x = -1.7$ and $M_y = -0.7$ m^{-1}/W, so that the calculated diameter of the laser mode in the epitaxial layer is $2w_L = 224 \pm 10$ μm and on the SESAM it is $2w_L = 144 \pm 10$ μm (within the studied range of P_{abs}). In this way, a kind of dynamically stable cavity was designed.

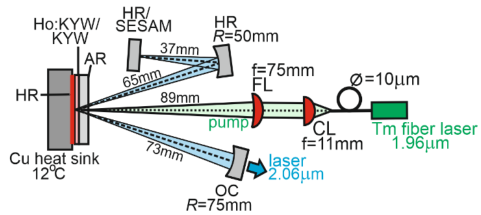

Fig. 1. Scheme of the PQS Ho:KYW thin-disk laser: OC – output coupler, HR – highly-reflective mirror, CL and FL – collimating and focusing lenses, respectively.

The pump source was a Tm-fiber laser (model IFL15, LISA Laser Products, OHG) emitting up to 12.5 W at 1960 nm (linewidth: 1.5 nm, unpolarized emission, M^2 ~1) corresponding to in-band pumping of Ho^{3+}, the $^5I_8 \rightarrow {}^5I_7$ transition. Its output was collimated and focused into the laser element using a pair of AR-coated spherical CaF_2 lenses (focal lengths: $f_{CL} = 11$ mm, $f_{FL} = 75$ mm) which resulted a pump spot size $2w_p$ of 300 ± 10 μm, i.e., $2w_p > t$ (the criterion for the thin-disk laser is satisfied). Pumping at nearly normal incidence, the total absorption (single-bounce) was 14%.

The GaSb-based SESAM was grown by conventional solid source molecular beam epitaxy (MBE) using elemental In, Ga and Al and Sb_2 and As_2, see [18,19]. First, a GaSb buffer was grown on a (100) *n*-GaSb substrate followed by 18.5 pairs of a lattice-matched $AlAs_xSb_{1-x}$ / GaSb Distributed Bragg Reflector (DBR). The optical structure corresponded to an anti-resonant design at the operating wavelength. The structure consisted of two $In_xGa_{1-x}As_ySb_{1-y}$ QWs with a 10 nm barrier placed 50 nm below the surface. The two-layer (TiO_2/SiO_2) dielectric AR coating applied for 1900-2100 nm was meant to increase the modulation depth and reduce the recovery lifetime [19].

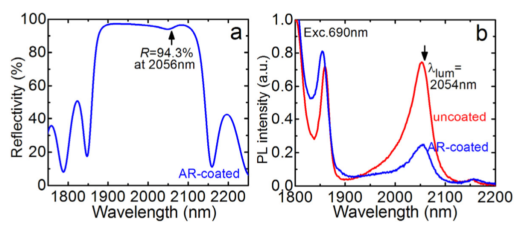

Fig. 2. Linear spectroscopy of the SESAM: (a) reflectivity spectrum (AR-coated sample); (b) photoluminescence (PL) spectra for uncoated and AR-coated samples, $\lambda_{exc} = 690$ nm, the *arrow* in (a,b) indicates the laser wavelength.

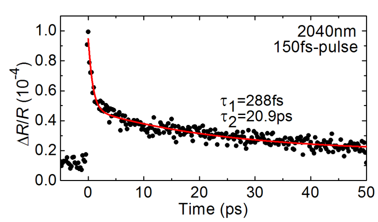

Fig. 3. Pump-probe trace for the uncoated SESAM measured at 2040 nm: *symbols* – experimental data, *curve* – their bi-exponential fit to determine the recovery times, $\tau_{1(2)}$. R and ΔR: reflectivity and its change, respectively.

The reflectivity spectrum of the AR-coated SESAM is shown in Fig. 2(a). A weak absorption band spanning from 2020 to 2080 nm is observed. The measured reflectivity at the laser wavelength ($\lambda_L = 2056$ nm) is 94.3% and the small-signal resonant absorption loss (for a single-bounce) is about 3.0%, as estimated from Fig. 2(a). The SESAM was also studied by luminescence spectroscopy, Fig. 2(b), showing a broad emission band centered at 2054 nm whose intensity was suppressed by the AR coating.

The recovery of the initial absorption of the SESAM was studied by the pump-probe method, Fig. 3. The source was the idler emission from a Spectra Physics Opal OPO tuned to 2040 nm (pulse duration: 150 fs, pulse energy: 2 nJ, the estimated pulse fluence: < 50 μJ/cm^2). The measured curve is fitted using a bi-exponential dependence with the characteristic "fast" and "slow" times τ_1 = 288 fs and τ_2 = 20.9 ps related to the intraband and interband relaxations, respectively.

3. Results and discussion

At first, the CW performance of the Ho:KYW TDL was studied by replacing the SESAM by the flat HR-mirror, Fig. 4(a). This laser generated a maximum output power of 592 mW at 2056-2059 nm (multi-peak emission, see Fig. 4(b)) with a slope efficiency η = 47% (with respect to P_{abs}). The laser threshold was at P_{abs} = 0.15 W. These results are slightly inferior with respect to the CW Ho:KYW thin-disk laser reported in [24] and based on a simple linear plano-concave cavity. The reason for this is less efficient mode-matching which can be optimized in further designs.

Implementing the SESAM, very stable Q-switching was observed. The maximum average output power reached 551 mW at 2056.3 nm (a single-peak spectrum, Fig. 4(b)) corresponding to a η of 44% and a Q-switching conversion efficiency with respect to the CW regime as high as 93%. In both CW and PQS regimes, the laser output was linearly polarized ($E \parallel N_m$), the polarization was naturally-selected by the anisotropy of the gain.

The output beam of the PQS laser was elliptic, see inset in Fig. 4(a), with measured $M^2_{x(y)}$ factors of 3.0 and 1.8, respectively (at P_{abs} = 1.40 W). The distortion of the laser beam is due to the strongly anisotropic thermal lens in the ***b***-cut Ho:KYW (the astigmatism degree, $S/M = |M_x - M_y|/|M_x|$ = 85%). The input-output dependences of both the CW and PQS lasers were linear indicating no detrimental influence of the thermal effects.

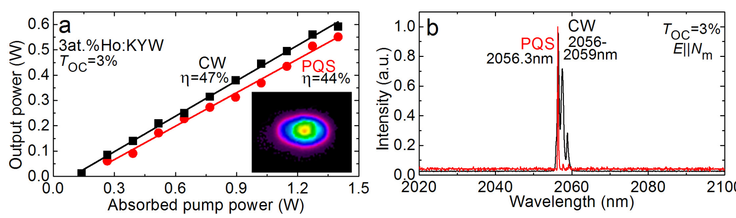

Fig. 4. CW and PQS Ho:KYW TDLs: (a) input-output dependences, η – slope efficiency, *inset*: spatial profile of the output beam for the PQS laser, P_{abs} = 1.40 W, (b) typical laser emission spectra measured at P_{abs} = 1.40 W, T_{OC} = 3%.

The pulse duration, $\Delta\tau$, determined as FWHM, and the pulse repetition frequency (PRF), were measured directly. The pulse energy E_{out} was calculated as P_{out}/PRF and the peak power P_{peak} – as $E_{out}/\Delta\tau$, see Fig. 5. The pulse energy increased with P_{abs} from 1.2 to 4.1 μJ and the duration shortened from 342 to 201 ns. This shortening was accompanied by an increase of the PRF in the range of 52-135 kHz. The maximum P_{peak} reached 20 W.

The dependence of the pulse characteristics on the pump power is typical for "fast" saturable absorbers [26] (as the recovery time of the GaSb-based SESAM is much shorter than the time of the pulse formation in the PQS laser) and related to a dynamic bleaching of the SA. No damage of the SESAM was observed. The calculated peak on-axis intracavity laser intensity on the SESAM, $I_{in} = X^*2E_{out}/(\pi w_L^2 \Delta\tau^*)$, where $X = (2-T_{OC})/T_{OC}$ and $\Delta\tau^* \approx 1.06\Delta\tau$ for Gaussian pulse assumption reached 6.4 MW/cm^2.

Typical oscilloscope traces of the pulsed output from the PQS laser are shown in Fig. 6. The single Q-switched pulses had a nearly Gaussian temporal shape, Fig. 6(a). The pulse train, see Fig. 6(b), exhibited low intensity instabilities (<10%) and rms pulse-to-pulse timing jitter (<7%). The long-term (>1 h) stability was also excellent.

Optics EXPRESS

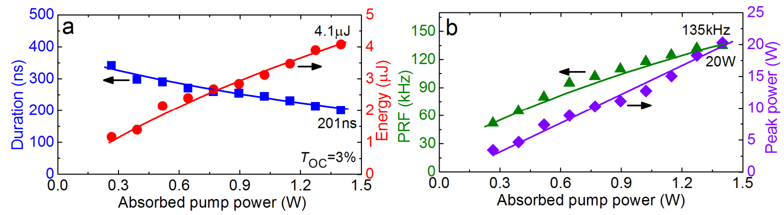

Fig. 5. PQS Ho:KYW TDL: pulse duration (FWHM) and pulse energy (a), pulse repetition frequency (PRF) and peak power (b).

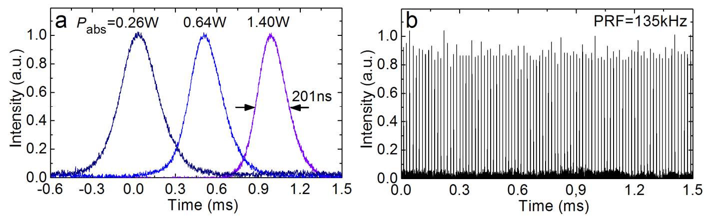

Fig. 6. Oscilloscope traces of the single Q-switched pulses captured at various P_{abs} (a) and the corresponding pulse train at P_{abs} = 1.40 W (b) for the PQS Ho:KYW TDL.

Further power scaling of the Ho:KYW PQS TDL is expected by the optimization of the Ho^{3+} doping level (1-5 at.%), thickness of the active layer, and an increase of the laser and pump spot size. The latter will help to improve the beam quality as the sensitivity factor of the thermal lens $M \sim 1/w_p^2$. As for the PQS output, shortening of the Q-switched pulses is feasible with a reduction of the cavity length and, thus, the cavity roundtrip time. The variation of the modulation depth of the SESAM (e.g., by varying the number of QWs) might lead to the increase of the pulse energy.

4. Conclusion

In conclusion, we report on the first Ho:MDT PQS TDL employing a 250 μm-thick 3 at.% Ho:KYW/KYW epitaxy as a laser element and a specially designed GaSb-based SESAM as Q-switch element. Relying on the ultimate simplicity of a single-bounce pump geometry, this laser generated more than 0.5 W of PQS output corresponding to very stable 4.1 μJ / 201 ns pulses at high repetition rate, 135 kHz. The successful application of GaSb-based SESAMs for stable Q-switching of such lasers is promising for the realization of compact few-ns PQS micro-lasers operating at high repetition rates as well as ML or Q-switched ML TDLs. For a small T_{OC} of 1.5%, we observed modulation of the Q-switched envelope with the cavity mode spacing of 0.86 GHz, i.e. longitudinal mode-beating. We believe that CW ML regime of the Ho:KYW TDL will be possible with an optimized cavity design.

Funding

Spanish Government (MAT2016-75716-C2-1-R (AEI/FEDER,UE), TEC 2014-55948-R), Generalitat de Catalunya (2014SGR1358).

Acknowledgments

F.D. acknowledges additional support through the ICREA academia award 2010ICREA-02 for excellence in research. X.M. acknowledges support from the European Union's Horizon 2020 research and innovation programme under the Marie Skłodowska-Curie grant agreement No 657630. P.L. acknowledges financial support from the Government of the Russian Federation (Grant 074-U01) through ITMO Post-Doctoral Fellowship scheme.